Predicting the effect of build orientation and process temperatures on the performance of parts made by fused filament fabrication

Fernando Moura Duarte and José António Covas
Institute for Polymers and Composites (IPC) Department of Polymer Engineering, University of Minho, Guimarães, Portugal, and
Sidonie Fernandes da Costa
Center for Research and Innovation in Business Sciences and Information Systems School of Management and Technology (ESTGF) of Porto Polytechnic Institute (IPP), Felgueiras, Portugal

Abstract

Purpose – The performance of the parts obtained by fused filament fabrication (FFF) is strongly dependent on the extent of bonding between adjacent filaments developing during the deposition stage. Bonding depends on the properties of the polymer material and is controlled by the temperature of the filaments when they come into contact, as well as by the time required for molecular diffusion. In turn, the temperature of the filaments is influenced by the set of operating conditions being used for printing. This paper aims at predicting the degree of bonding of realistic 3D printed parts, taking into consideration the various contacts arising during its fabrication, and the printing conditions selected.

Design/methodology/approach – A computational thermal model of filament cooling and bonding that was previously developed by the authors is extended here, to be able to predict the influence of the build orientation of 3D printed parts on bonding. The quality of a part taken as a case study is then assessed in terms of the degree of bonding, i.e. the percentage of volume exhibiting satisfactory bonding between contiguous filaments.

Findings – The complexity of the heat transfer arising from the changes in the thermal boundary conditions during deposition and cooling is well demonstrated for a case study involving a realistic 3D part. Both extrusion and build chamber temperature are major process parameters.

Originality/value – The results obtained can be used as practical guidance towards defining printing strategies for 3D printing using FFF. Also, the model developed could be directly applied for the selection of adequate printing conditions.

Keywords 3D printing, Bonding, Cooling, Build orientation, Fused filament fabrication FFF

Paper type Research paper

1. Introduction

Additive manufacturing (AM) techniques differ from the traditional subtractive manufacturing route, as the product is built into the desired shape following a "layer-by-layer" approach. Alghamdi *et al.* (2021) reviewed recently the progress, promise and challenges of AM techniques for polymers. Among them, fused filament fabrication (FFF) uses continuous filaments of thermoplastic materials or composites to gradually build 3 D parts layer by layer, which can exhibit substantial geometrical complexity. FFF comprises the trademarked fused deposition modeling (FDM), which uses a previously manufactured filament, and free form extrusion (FFE), which converts directly polymer pellets into the thin filament that is printed. FFF is assuming an increasingly important role in the portfolio of manufacturing techniques not using a shaping mould due to its easy operation, reproducibility, low cost and suitability to work with a range of materials (Chua *et al.*, 2010). FFF can produce prototypes for concept validation during the design phase (Ingole *et al.*, 2009), as well as final parts with advanced functionalities, e.g. with gradient properties by combining several polymer materials (Harris *et al.*, 2019). Moreover, 4D printing combines 3D printing with time to yield printed components that respond to external stimuli, changing their shape/volume or modifying their mechanical properties (Valvez *et al.*, 2021).

In line with other authors, Mackay (2018) demonstrated that FFF involves heating and melting, flow, bonding and solidification/cooling processes. Therefore, the performance of parts, namely, their mechanical properties, surface roughness and

The current issue and full text archive of this journal is available on Emerald Insight at: **https://www.emerald.com/insight/1355-2546.htm**

Rapid Prototyping Journal

[DOI 10.1108/RPJ-04-2021-0084]

Funding: This work is funded by National Funds through FCT – Portuguese Foundation for Science and Technology, References UIDB/05256/2020, UIDP/05256/2020 and UIDB/04728/2020.

Partial support for this research has been provided by the Search-ON2: Revitalization of HPC infrastructure of UMinho, (NORTE-07–0162-FEDER-000086), co-funded by the North Portugal Regional Operational Programme (ON.2-O Novo Norte), under the National Strategic Reference Framework (NSRF), through the European Regional Development Fund (ERDF), at the University of Minho, Portugal.

Received 15 April 2021
Revised 26 May 2021
3 September 2021
Accepted 5 October 2021

dimensional tolerances, is strongly influenced by the bonding between adjacent filaments. For example, Li *et al.* (2018) observed that the tensile strength is closely related to interface bonding, and that layer thickness governs bonding strength and, therefore, strongly affects the mechanical behavior of the printed parts. Wang *et al.* (2019) modelled surface roughness considering the diffusion between filaments and concluded that it decreases with increasing nozzle and platform temperatures. Striemann *et al.* (2020) used an infrared preheating system to maintain the temperature of the interlayer zone above the glass transition temperature during the deposition stage and obtained a 15% increase of the tensile strength. Céline *et al.* (2004) estimated the dynamics of bond formation from sintering data of Acrylonitrile Butadiene Styrene (ABS) filaments, while Gurrala and Regalla (2014) analysed changes in the mesostructure and degree of bonding at the interfaces between adjoining polymer filaments. Recently, Liparoti *et al.* (2021) showed that a successful diffusion and re-entanglement of the polymer across the interfaces of adjacent layers are the key to ensure the strength of the final printed part. Therefore, the required molecular diffusion for bonding depends on the rheological properties of the polymer material and on the local temperatures and associated times. These depend on the heat transfer during filament deposition (i.e. the printing stage of the process) and cooling. Furthermore, because polymers are generally thermal insulators, large temperature gradients develop during deposition, resulting in the creation of residual stresses. As explained by Rudolph *et al.* (2019), these may initiate warpage and delamination.

The temperature evolution of the filaments in FFF has been studied both theoretically and experimentally. Yardimci and Güceri (1996) and Yardimci *et al.* (1997) modelled the cooling of a single filament due to convection with the environment (i.e. disregarding physical contacts) and showed the effect of adopting different build strategies. More recently, Zhou *et al.* (2017) used the ANSYS 17.2 commercial software to introduce the effect of the contact of the filament with the build platform. Rudolph *et al.* (2019) and D'Amico and Peterson (2018) modelled the cooling of vertical filament stacks. These two approaches also used commercial software by using element death and birth effects to represent the addition of polymer during the deposition process. Rudolph *et al.* (2019) considered the existence of voids between adjacent filaments, and by employing ANSYS concluded that the dimension of the voids has a great influence on the rate of reheating and cooling. D'Amico and Peterson (2018) used Multiphysics® simulation software (COMSOL's) "Deformed Geometry" nodes and found good agreement with the experimental data. Costa *et al.* (2017) took into consideration the various possible physical contacts between any filament and its neighbours (or the build platform of the 3D printer) during the printing stage, thus enabling predicting the temperature evolution in practical 3D parts manufactured under pre-defined processing conditions. This approach was recently incorporated by Garzon-Hernandez *et al.* (2020) in their proposed modelling methodology for the calculation of the mechanical performance of FDM components, which included a sintering model and theoretical expressions to predict void density and mechanical properties. Zhang and Shapiro (2018) developed a thermal model similar to that of Costa *et al.* (2017), which can be applied directly on the geometry described by a typical manufacturing process plan, but assuming 100% degree of fill.

Experimental measurements of temperature in FFF are challenging due to the additive nature of the process and the small filament diameters (typically 0.1–0.3 mm), making more difficult to position sensors. Readings of filaments temperature by direct contact call for small sensors (sizes of few tens of micrometre) to minimize interference with the deposition process. For example, Kousiatza and Karalekas (2016) used fibre Bragg grating sensors to measure strain and temperature. They observed that temperature peak values were generated when new filaments were deposited. Similar conclusions were made when positioning a thermocouple between layers (Kousiatza *et al.*, 2017). Infrared thermography provides non-contact sensing, and as such has been frequently adopted for FFF. Seppala and Migler (2016) measured the temperature evolution of a vertical stack of 8 layers of ABS filaments. They observed that the temperature of each printed layer decreased at a rate of approximately 100°C/s, remaining above the glass transition temperature for approximately 1 s. Wolszczak *et al.* (2018) used a thermal imaging camera equipped with a macro lens to measure the temperature distribution of the surface of the test piece. They confirmed that the temperature of a given layer increases when a new layer is deposited on top of it. Other authors adopted thermography to assess theoretical predictions of temperature evolution during printing and cooling. Ravoori *et al.* (2019) measured the temperature field of a PLA filament deposited on the build platform, and concluded that thermal diffusion to the bed and heat transfer from the hot nozzle tip influence the temperature distribution. Ferraris *et al.* (2019) developed an infrared based set-up capable of capturing spatial and temporal variations of temperature during printing and used the experimental results to validate a thermal numerical model.

The spatial and temporal temperature fields developing during printing depend on the processing parameters selected, such as extrusion, build chamber and build platform temperatures, printing velocity, fill strategy, build orientation, nozzle diameter, filament diameter, layer thickness, raster angle, etc. Build (or part) orientation, i.e. the rotation of the part in the manufacturing space around the axes of the machine coordinate system, affects the thermal history imposed (Leutenecker-Twelsieka *et al.*, 2016). For example, Faes *et al.* (2016) observed experimentally for ABS components that the time interval between printing two consecutive layers in a given part, which depends on the fabrication strategy, correlated inversely with the mechanical properties in the vertical direction. Similarly, it was found that horizontal and vertical printing influenced the overall mechanical behavior of parts printed by FDM. Plaza *et al.* (2019) demonstrated the strong effect of build orientation of a small parallelepiped (80 × 10 × 4 mm) PLA on the dimensional accuracy, flatness and surface texture, using a low cost open-source FFF 3 D printer. Cole *et al.* (2016) investigated the influence of the build orientation on the multiscale mechanical behavior of dog bone test specimens printed by FDM. While the Young's modulus was fairly consistent for the various orientations, tensile strength varied significantly. Malekipoura *et al.* (2018) also tested dog bone test specimens, but monitored the effect of build orientation on the temperature evolution of the part. They suggested that printing conditions creating a more even spatial temperature would also yield better mechanical properties.

This work aims at extending the current understanding of the effect of build orientation and process temperatures (i.e. extrusion, build chamber and build platform temperatures) on the performance of parts produced by FFF. The approach here is to establish generic correlations between process parameters and the resulting spatial and temporal temperature fields which, in turn, determine the quality of bonding between filaments. The heat transfer and bonding model previously developed by the authors (Costa *et al.*, 2017) is upgraded to be able to make computations for different build orientations. Then, in silico experiments yield predictions of temperature and bonding for an illustrative 3D part that is printed using various processing conditions.

2. Modeling heat transfer and bonding

Filament cooling is a transient process that is influenced by heat transfer with the build platform, build chamber and with adjacent filaments (Costa *et al.*, 2014), as well as by the crystalline or amorphous nature of the polymer (Costa *et al.*, 2020). The MATLAB computer code used here considers the heat transfer modes taking place during the gradual deposition of the filament while activating the relevant thermal boundaries at each time step, depending on the geometry of the part, build orientation, filling strategy adopted and degree of fill (a detailed description of the algorithm is available in (Costa *et al.*, 2017; Costa *et al.*, 2015; Costa *et al.*, 2011). As illustrated in Figure 1, the thermal conditions may encompass conduction with the build platform of the 3 D printer or with contacting filaments (in the lower, same, or upper layer), or convection (natural or forced), whereas radiation is not taken into consideration due to its smaller effect (Costa *et al.*, 2014). The predictions obtained with the model were shown to be generally in good agreement with experimental data (Vanaei *et al.*, 2020). Also, as represented in Figure 1, taking advantage of the calculation of the spatial and temporal temperature fields, the code also predicts the degree of bonding within the part between adjacent filaments either in the same layer or in different layers, by applying the healing criterion proposed by Yang and Pitchumani (2002) that is based on a fundamental formulation of the reptation of polymer chains:

$$D_h(t) = \left[\int_0^t \frac{1}{t_w(T)}dt\right]^{1/4} \quad (1)$$

where $t_w(T)$ is the welding time. Bonding develops when $D_h(t) \geq 1$. $t_w(T)$ is obtained experimentally (Rodriguez *et al.*, 2000; Sun, 2003). Rodriguez *et al.* (Rodriguez, 1999) performed fracture tests at room temperature on FDM parts made of ABS that were subjected to three different temperatures (118°C, 125°C, 134°C) and healing times ranging from 1 min to 8 h. An Arrhenius equation was then used to correlate the welding time with temperature:

$$t_w = 1.080 \times 10^{-47} \exp\left(\frac{Q_d}{RT}\right) \quad (2)$$

where Q_d=388°700J/mol, R is the specific gas constant for air (J/mol K) and T is temperature (K).

The above heat transfer model is quite general; its applicability is dependent on the availability of the thermo-physical properties of the polymer or composite to be printed. Also, the knowledge of the temperature evolution with time of the various filaments could be used to carry out other predictions, such as shrinkage, residual stresses and warpage, but these are outside the scope of the present study.

Figure 2 illustrates the influence of the physical contacts between filaments on cooling. An ABS filament is extruded at 270°C, at the speed of 0.025 m/s, inside a build chamber kept at 70°C, to obtain the simple parallelipipedic geometry shown in Figure 2a, with the deposition sequence indicated by the numbers identifying each filament. Considering the transversal vertical plan also represented in the Figure 2a, the various individual filaments will progressively cool down as pictured in Figure 2b. The deposition of one filament affects the cooling of those that were deposited previously, i.e. when a new filament is printed, the previously deposited filament(s) that is(are) contacted is(are) re-heated. In this example, these physical contacts can alter the local filament temperatures by as much as 24°C. In some cases (Filaments 2–9), filaments are re-heated above the glass transition temperature of ABS (represented by the horizontal solid red line), which is a major threshold required for bonding. Even cooling of Filament 1, the first to be laid, is affected by the deposition of the remaining 11 filaments, although only Filaments 2 and 8 are in contact with it. This example demonstrates that studies involving simple vertical stacks of filaments cannot fully capture these important thermal phenomena.

The algorithm that was previously developed has limitations in terms of the geometries that can be analysed, preventing the investigation of the effect of the build orientation on cooling, which is the main aim of the present work. The geometry to be defined is enveloped in a parallelepiped volume, which is filled by real or virtual filaments of equal length. In the example illustrated in Figure 3a, the part is printed with filaments deposited along its width. The real filaments (coloured grey) are assigned with the value of 1, whereas the virtual ones (no color) have value 0. A 2D matrix $M \in \mathcal{M}_{m\times n}$, where m is the number of layers and n is the maximum number of filaments in one layer, is then built. To provide greater geometrical freedom to the part and simultaneously enable the definition of filaments with different lengths, a new approach was adopted. Now, as seen in Figure 4b, the volume enveloping the part is discretized into elementary parallelepiped volumes, which are assigned with the value of 1 or 0, depending on the existence of polymer or air, respectively. The corresponding 3D matrix $M \in \mathcal{M}_{m\times n\times p}$, where m is the number of layers, n is the maximum number of filaments in one layer and p is the maximum number of elementary volumes along the length of the filaments, is then defined.

The thermal computations are performed as the part is progressively printed. This means that during this process it is necessary to define the time increments at which the thermal conditions must be up-dated. When the filaments have the same length, this is relatively straightforward, each filament being divided into a number of axial increments and an analytical expression for time updating is derived. When the individual filaments constituting the part have different lengths, such an expression no longer exists. Now, a specific algorithm

Figure 1 General flowchart of the computer code used in this study

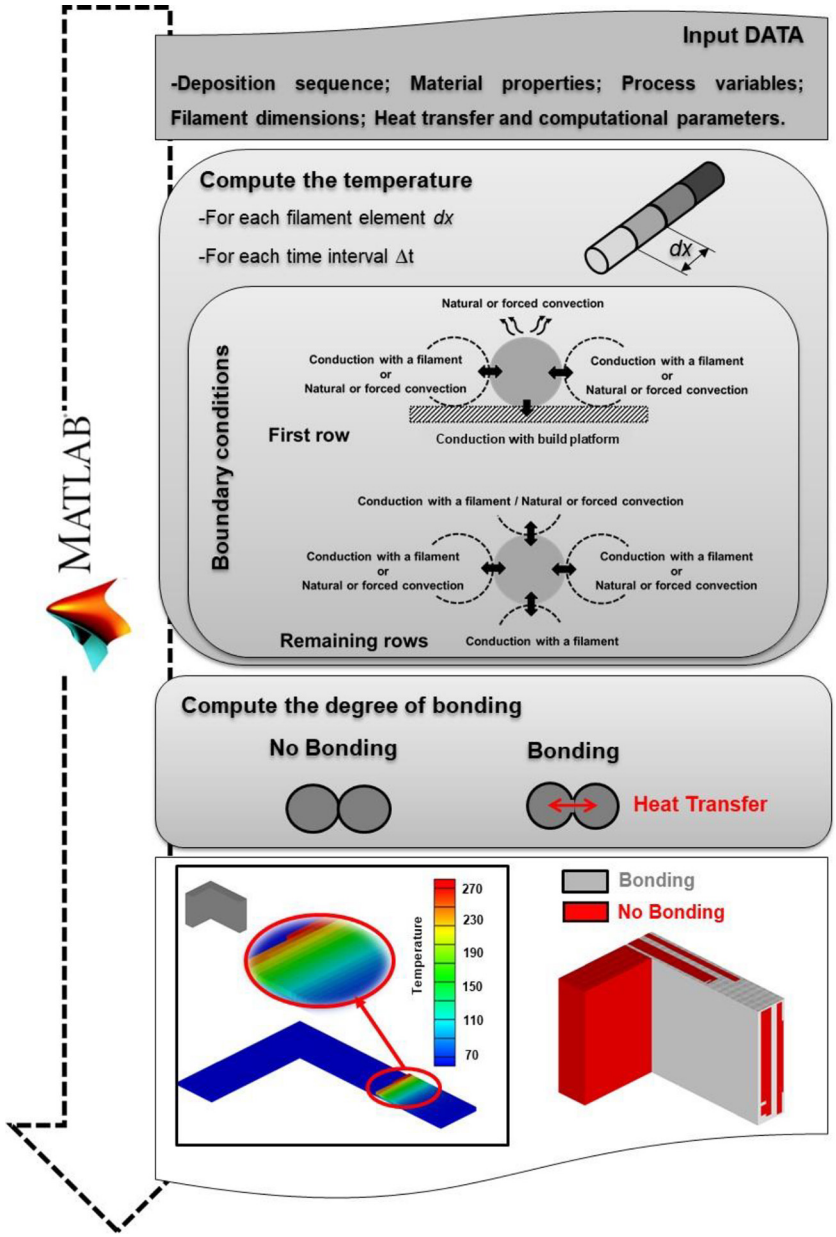

to determine the updating times is necessary. This algorithm runs prior to the thermal computations, following the deposition path that will be followed to build the part and identifying all the updating times.

3. 3D Part and printing parameters

The geometry and dimensions of the part to be printed are presented in Figure 4. In principle, six different build orientations are possible, as schematized in Figure 5 (and labelled a to f). As shown in the Figure 5, orientations E and F will require the use of a second material to build a support structure, but this can be handled by the software in terms of its contribution to the heat transfer. Indeed, as the support structure is also deposited, a bi-material 3D printing process must be considered, where the temperatures of the filaments of the support structure are also computed and will influence the temperature history of the filaments of the part.

Although it is not possible to ignore the effect of the heat transfer of the supporting structure on the total heat transfer, which may bias the direct comparison between the results for orientations E and F with the remaining, these two orientations are included in the analysis as they are two valid construction options (despite of their obvious greater printing time and manufacturing cost). Additionally, the addition of orientations E and F in the study allows to evaluate the influence of the supporting structure on the temperature and bonding of the part.

An unidirectional and aligned deposition sequence, and 100% degree of fill were chosen. However, other deposition

Figure 2 Influence of the physical contacts on temperature evolution during filament deposition

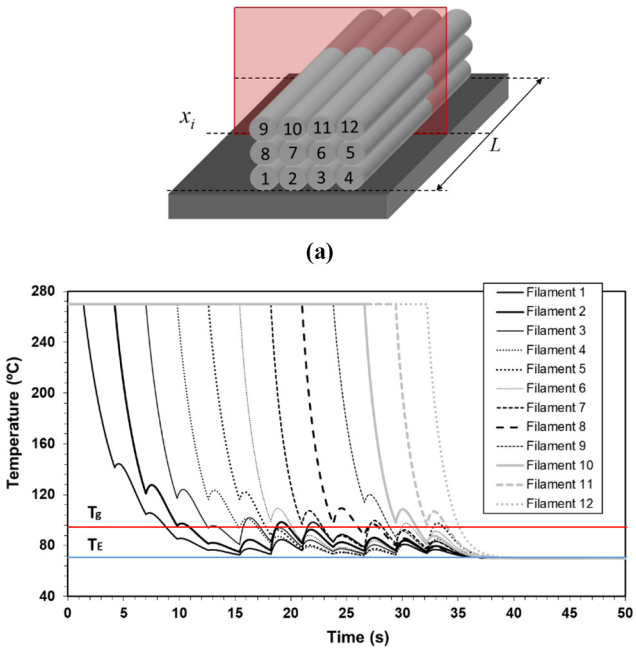

Notes: (a) Geometry to build and sequence of filament deposition; (b) temperature evolution. Tg – glass transition temperature; TE –temperature of the build chamber

Figure 3 Definition of the geometry of a part for the thermal computations

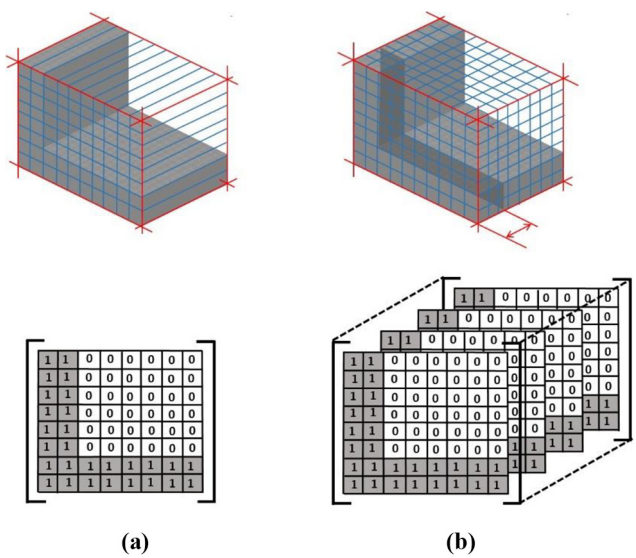

Notes: (a) In the previous heat transfer model all filaments have equal length (in this case, equal to the width of the part), hence a 2D matrix is built considering the existence (value 1) or inexistence (value 0) of a filament in the volume enveloping the part; (b) in the new model, the volume enveloping the part is discretized into elementary volumes, and a 3D matrix is build considering the local existence (value 1) or inexistence (value 0) of polymer

Figure 4 Geometry and dimensions of the part studied

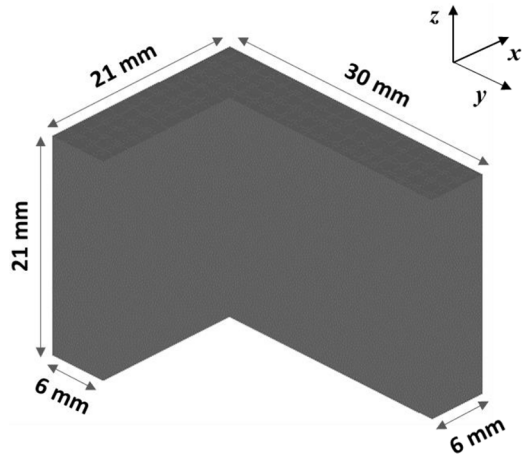

sequences and degrees of fill could be taken. Neck growth of the filament upon deposition is not considered; a constant value is assumed once the filaments contact each other and until printing is complete. Therefore, for a filament with a diameter of 0.4 mm (nozzle diameter), simple volume calculations reveal that orientations A to D involve the deposition of 3000 filament segments, while orientations E and F are built from 7,000 filament segments (of the two materials). Obviously, this will correspond to different manufacturing times, which are estimated as 42 min for orientations A to D and 98 min for E and F.

Table 1 presents the main properties of the materials. The part is made of ABS (P400 ABS, Stratasys®), while PLA (881 N PLA, Filkemp®) is the support material. The former is an amorphous polymer, while the latter is partially crystalline. For build orientations E and F predictions of bonding are only made for ABS, since PLA is to be subsequently discarded. However, as discussed above, temperature computations must be performed for both, as they are in contact. Table 2 identifies the reference values of the process parameters. The existence of a forced convection oven (build chamber) is assumed by default. The computations were performed considering time increments of 0.012 s and a temperature convergence error of 1°C.

4. Results and discussion

Figure 6 shows predictions of bonding quality (in terms of locations and volume fraction of the part exhibiting no or insufficient bonding) when the part under study is printed using different extrusion temperatures and adopting the various possible build orientations. Bonding is estimated by the healing criterion proposed by Yang and Pitchumani (2002) which, as explained above, considers the local temperature and corresponding time interval as major parameters ruling the required molecular diffusion. At 270°C (typical extrusion temperature for ABS that is automatically adopted by most commercial 3 D printers) all parts exhibit good quality. Bonding problems arise and intensify with decreasing extrusion temperature. When the filament is extruded at 250°C, the printed parts should exhibit little mechanical resistance, as the individual filaments are poorly bonded to each other. This

Figure 5 Deposition sequence (unidirectional and aligned) and possible build orientations for the part illustrated in Figure 4

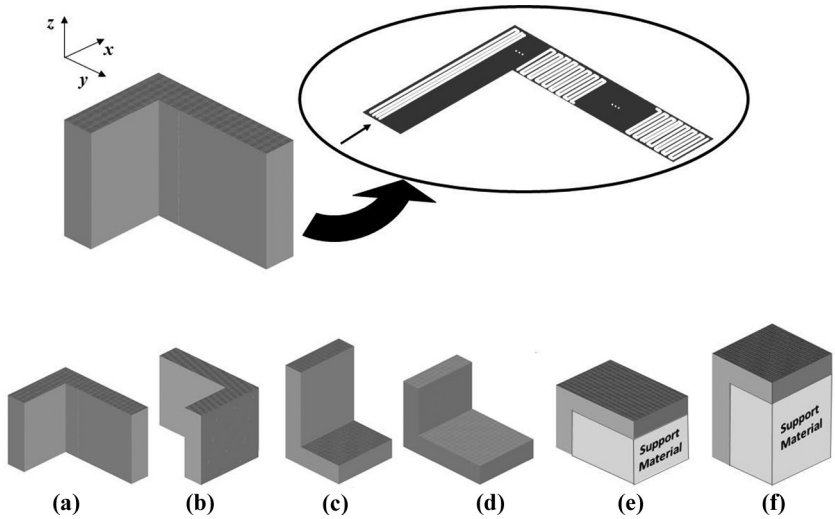

Table 1 Materials properties

Property	ABS P400	PLA
Density, ρ (kg/m^3)	1050	1300
Thermal conductivity, *k* (W/m °C)	0.18	0.2
Specific heat, *Cp* (J/kg °C)	2020	2100
Glass transition temperature, T_g (°C)	94	60

result was obviously anticipated qualitatively, as the extrusion temperature decreased the various filaments stay above the glass transition temperature during shorter times.

Figure 6 also reveals significant differences in bonding for the various build orientations at equal extrusion temperature. Orientations A and B display the poorer performance. This can be clearly observed in Figure 7, which displays the correlation between bonding and extrusion temperature for the various build conditions. Orientations A and B require 5°C–8°C higher extrusion temperature to yield parts with the same quality as that obtained with the remaining build orientations. These differences arise due to disparities in the deposition process associated to each build orientation. As can be seen in Figure 5, at each XY plan, orientations A and B entail the deposition of long filament segments followed by short filament segments in each layer, and vice-versa, respectively. Conversely, all the remaining build orientations involve the deposition of filament segments of equal length. At constant extrusion velocity, contacts between long filament segments arise at higher time intervals. Thus, those filaments are likely to cool down faster, as re-heating due to contacts with newly deposited filament segments takes longer. This phenomenon is further demonstrated in Figure 8. The figure presents four snapshots at different times (10, 30, 45 and 75 s) along the deposition sequence for build orientation A. At 10 s (Figure 8a), the short side of the first layer is being printed by means of long filament segments. At 30 s (Figure 8b), the long side of the first layer is being printed, involving the deposition of short filament segments. At 45 s (Figure 8c), the first layer is completed and the second layer of the long side is now being printed. It can be seen that the newly deposited filament segments re-heat the colder segments of the first layer to temperatures above 120°C, i.e. above the glass transition temperature of ABS (94°C, Table 1), during sufficient time to enable good bonding between them. Contrariwise, at t = 75 s (Figure 8d), the new filaments of the second layer are unable to reheat meaningfully the previously deposited segments, as a long time elapsed since deposition, and thus cooling developed significantly.

Orientations E and F exhibit a thermal history similar to that of orientations C and D, respectively, having the same contact

Table 2. Reference process parameters

Property	Value
Extrusion temperature, T_L (°C)	270
Build chamber temperature, T_E (°C)	70
Build platform temperature, T_S (°C)	70
Deposition velocity, *v* (m/s)	0.025
Convective heat transfer coefficient, h_{conv} (W/m^2 °C)	65
Thermal contact conductance between filaments, h_i (W/m^2 °C)	[10^{-4}]
Thermal contact conductance between filaments and build platform, h_{sup} (W/m^2 °C)	10
Perimeter fraction of each contact, λ_i	0.25
Nozzle diameter, d (mm)	0.4
Layer thickness, α (mm)	0.3

Figure 6 Effect of build orientation and extrusion temperature, T_L, on the quality of bonding of the part studied ($T_E = 70°C$;$h_{conv} = 65°W/m^2s^2°C$; $h_{sup} = 10°W/m^2s^2°C$; $v = 0.025m/s$

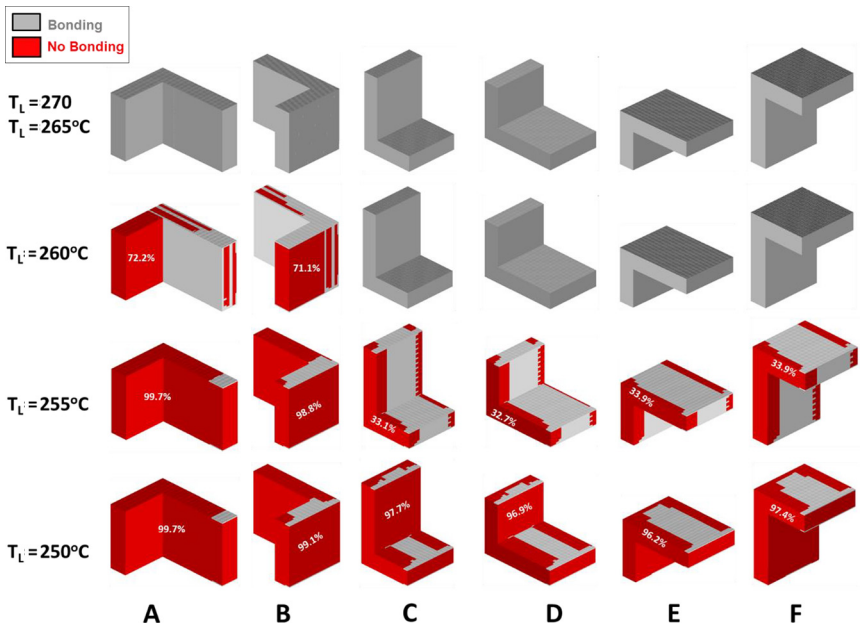

Figure 7 Effect of build orientation on the relationship between bonding quality and extrusion temperature, T_L

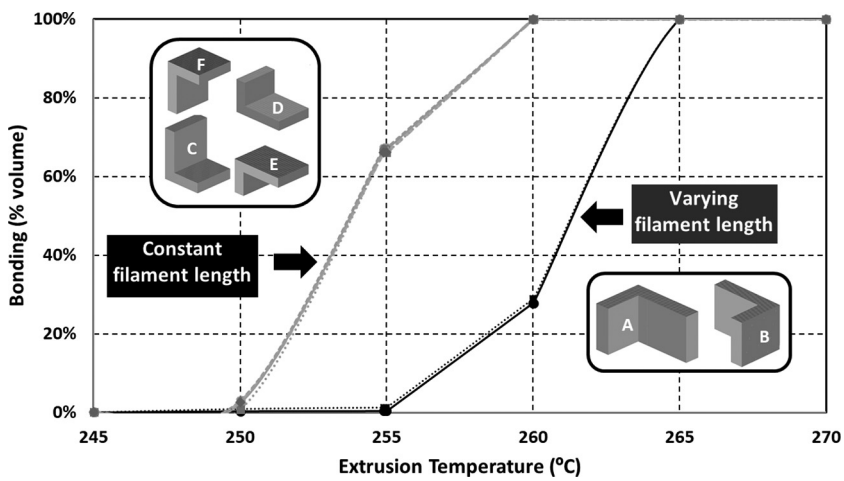

area with the build platform and a similar length of the printed filament. Therefore, contact area and filament length control the temperature evolution of the part, the presence of a support structure having a minor importance.

Another interesting feature of the bonding patterns seen in Figure 6 (e.g. at 260°C, for build orientations A and B) is the eventual development of regions alternating between bonding and no bonding. As discussed above, if two filaments become in contact with each other after a sufficiently long time has elapsed, bonding will most likely fail. This implies a small mutual contact area due to the limited material flow/deformation involved, and therefore little heat transfer between them. Consequently, the oldest filament re-heats only slightly, while the one just printed will remain hot. When a third filament contacts the latter, bonding could develop if the time elapsed is reasonably short. As bonding involves molecular diffusion between the two filaments, the contact area will become larger and heat transfer will be more effective. This means re-heating of the second filament and comparable cooling of the newest filament. Seppala *et al.* (2017) confirmed experimentally this temperature evolution for a vertical filament stack. Thus, when a fourth filament becomes in contact with the third filament, the associated elapsed time will determine whether bonding will develop or not. In more general terms, the lack of bonding between a pair of filaments prevents efficient heat transfer between them. This causes slower cooling of the most recent filament which can favour bonding with a newer filament. Conversely, when bonding develops between a pair of filaments, the greater heat transfer between them will promote faster cooling of the most recent one, which could deter bonding of the latter with a newer filament. Under constant

Figure 8 Evolution of the temperature of the filaments deposited during printing of the part studied using build orientation A (extrusion temperature, T_L= 260°C)

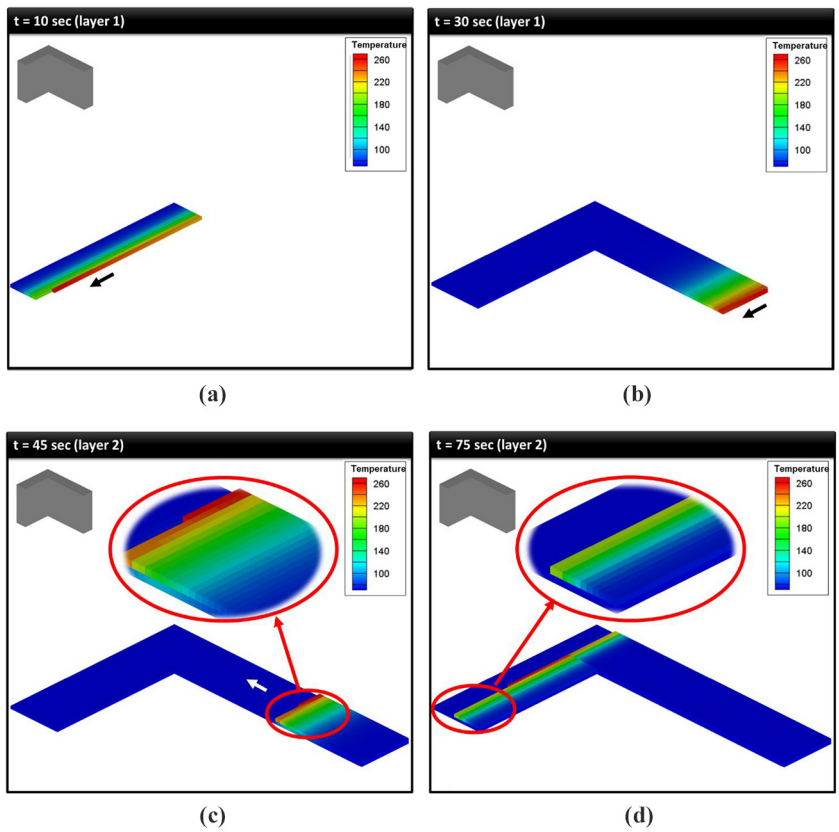

Notes: (a) *t* = 0s; (b) *t* = 30s; (c) *t* = 45s; (d) *t* = 75s

printing velocity, this mechanism is obviously governed by the geometry of the part.

The importance of the physical contacts between filaments in 3D printing by FFF is now evident, and the practical usefulness of predictive models such as the one proposed here is also demonstrated. For example, these models can support the selection of adequate processing temperatures, which are crucial to obtain good quality parts. Within this context, Figure 9 displays estimates of bonding quality when the part under study is printed at different build chamber temperatures, T_E, and using the various build orientations. As expected, lower build chamber temperatures are associated to poorer quality parts, as the filaments cool faster, thus hampering bonding. The correlation between bonding and build chamber temperature for the various build conditions is depicted in Figure 10. Similarly to the effect of extrusion temperature, orientations A and B require 5°C–8°C higher build chamber temperature to produce the part under study with similar quality as that obtained with build orientations C to F.

The option of using a 3D printer without a build chamber, but with the possibility of controlling the temperature of the build platform can also be explored. In this case, the convection heat transfer will be lower than that assumed in the above discussions, as cooling develops under natural convection conditions [typically, h_{conv} =30 W/m^2.°C, obtained from the Churchill and Chu's correlation (Holman, 2010)]. Also, the heat transfer between the filaments and the build platform can differ significantly, as support materials can vary (usually, glass or polymers are used), and, in some cases, the users modify the surface characteristics to guarantee the adhesion of the first printed layer onto the build platform. This is vital for printing but simultaneously should also facilitate the subsequent removal of the part without damaging it. For example, the printing surface may be covered with polymeric films or tapes, the tape surface can be made rougher by sanding it, and water-soluble glues, hair sprays or special coatings, may also be applied (Spoerk *et al.*, 2018). Concomitantly, increasing the temperature of the build platform to a recommended value for a given material is also commonly adopted. It has been shown that a significant increase in adhesion between the printed filaments and the build platform can be obtained when the latter is kept at a temperature slightly above the glass transition temperature of the polymer to be printed (Spoerk *et al.*, 2018). Figures 11 and 12 present the influence of the build platform temperature on the bonding quality of the printed part under study, for high (h_{sup} =150 W/m^2.°C) and low (h_{sup} =10 W/m^2.°C) conduction heat transfer coefficient values, for an extrusion temperature, T_L = 270°C, and the usual 6 build orientations (A to F). The two figures demonstrate that when printing at room temperature (under natural convection), build orientations A and B are not able to yield good quality parts, while the opposite tends to occur for the remaining orientations. If the heat transfer

Figure 9 Influence of build orientation and build chamber temperature, T_E, on bonding. $270°C; h_{conv} = 65°W/m^2s^{2o}C$; $h_{sup} = 10°W/m^2s^{2o}C$; $v = 0.025m/s$

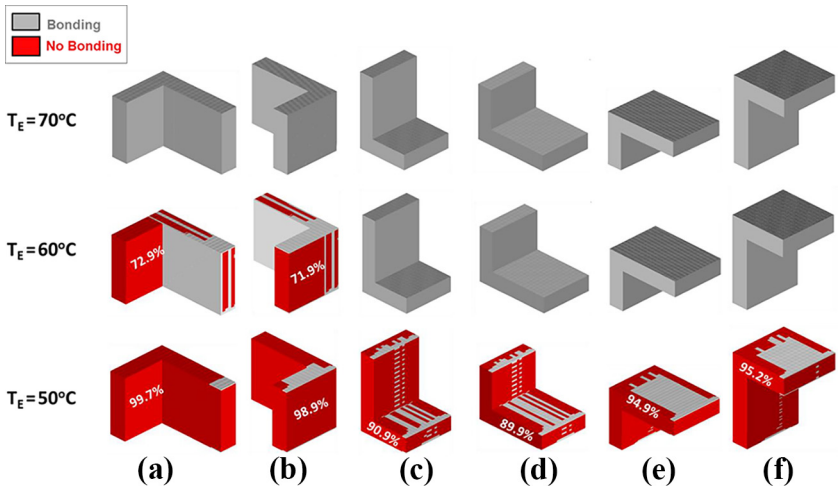

Figure 10 Effect of build orientation on the relationship between bonding quality and build chamber temperature, T_E

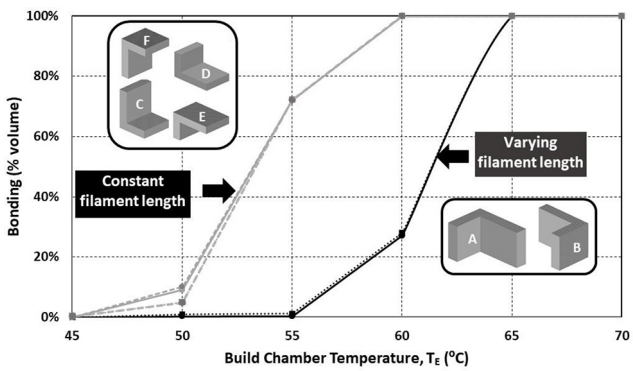

between the filaments and the build platform is high (Figure 11), the temperature of the build platform can have two contrasting effects on the cooling of the filaments: for temperatures up to 50°C, the build platform induces faster cooling of the filaments in the lower layers, and bonding problems may appear. For temperatures above, bonding is favoured for build orientations A and B, and all the remaining present good bonding. When the heat transfer between the filaments and the build platform is low (Figure 12), at low build platform temperatures the cooling effect is delayed, but at high temperatures the heating effect helping adhesion is smaller. In this case, while the bonding in parts A and B is inferior to that of equivalent parts produced under high conduction heat transfer, the remaining build orientations still exhibit good quality.

Again, the data show that orientations E and F behave similarly to C and D, respectively. This confirms the role of the contact area with the build platform and the length of the printing filament has major process parameters controlling the evolution of temperature and bonding.

The above results can be used to select the most adequate build orientation, extrusion, build chamber and build platform temperature, for the part under study. Build orientations A and B can be excluded, as they are more prone to generate bonding problems. Orientations E and F can also be discarded, since not only they are not advantageous from a bonding point of view when compared with orientations C and D, but they also require longer printing times and the use (and subsequent waste) of support material. When comparing build orientations C and D, the latter involves higher contact area between the part and the build platform, which is usually associated with the need of more post-processing operations (Dutta and Kulkarni, 2000) and often causes practical difficulties (discussed Above). Consequently, build orientation C seems the most favourable. Adequate extrusion and build chamber temperatures seem to be in the range 265 – 270°C and 65 – 70°C, respectively, and the build platform temperature, higher than 50°C.

Conclusions

The deposition and cooling process stages during 3D printing of a part using Fused Filament Fabrication involve a complex interplay between heat transfer and molecular diffusion for proper bonding between adjacent filament segments. Using heat transfer models that analyse the gradual deposition of the filament, while activating the relevant contacts at each process time step, it is possible to obtain a better understanding of the phenomena involved. Local temperatures and time for contact between adjacent filament segments govern the quality of bonding. Bonding requires that, upon contact, the new hot filament re-heats sufficiently the older filament (above its glass transition or melting temperature, depending on its amorphous or partially crystalline character), during the necessary time. Considering a representative 3D part, correlations were established between bonding quality and extrusion, build chamber and build platform temperatures, for various build orientations. Build orientation, extrusion and build chamber temperatures showed a strong influence on heat transfer. Also, better results are generally obtained when the part is constructed using filaments having similar lengths. Moreover, comparison of the thermal history of the various build orientations, revealed that the contact area with the build platform and filament length control the temperature evolution of the part.

Figure 11 Influence of build orientation and build platform temperature, T_{sup}, on bonding for high conductivity between the build platform and the filament ($h_{sup} = 150°W/m^2$). $T_L = 270°C$;$h_{conv} = 30\ W/m^2s^2°C$; $v = 0.025m/s$

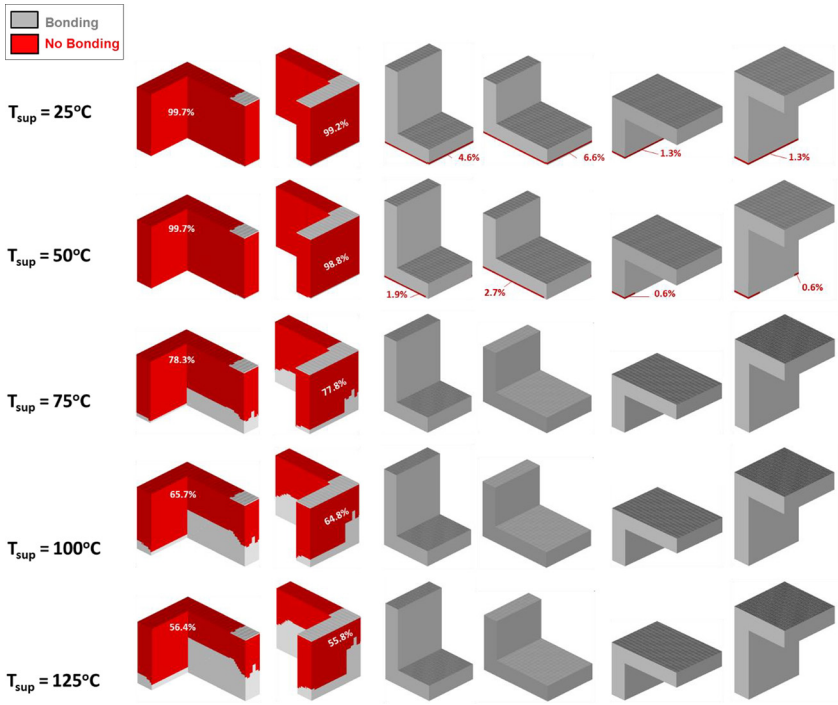

The predictions provided by the proposed heat transfer model can be used for the selection of the most favourable build orientation of a given part, as well as for the definition of the operating conditions yielding better bonding. The model can be applied for amorphous or semi-crystalline materials, in which case a phase change must be considered. Obviously, any polymer system can be considered as long as its thermo-physical properties are known, including its welding time.

Figure 12 Influence of build orientation and build platform temperature, T_{sup}, on bonding for low conductivity between the build platform and the filament ($h_{sup} = 10°W/m^2s^2°C$). $T_L = 270°C$;$h_{conv} = °30\ W/m^2s^2°C$; $v = 0.025m/s$

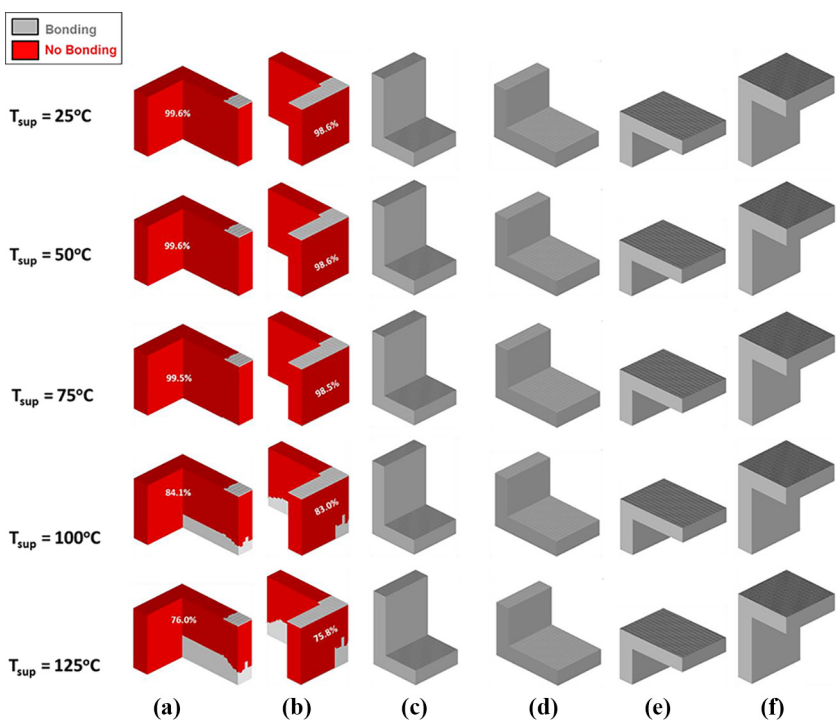

Finally, the temperature evolution with time provided by the model can be used as input for predictions of residual stresses, warpage and mechanical performance of printed parts.

References

Alghamdi, S.S., John, S., Choudhury, N.R. and Dutta, N.K. (2021), "Additive manufacturing of polymer materials: progress, promise and challenges", *Polymers*, Vol. 13 No. 5, p. 753, doi: 10.3390/polym13050753.

Céline, B., Longmei, L., Sunj, Q. and Gu, P. (2004), "Modelling of bond formation between polymer filaments in the fused deposition modelling process", *Journal of Manufacturing Processes*, Vol. 6 No. 2, pp. 170-178, doi: 10.1016/S1526-6125(04)70071-7.

Chua, C.K., Leong, K.F. and Lim, C.S. (2010), *Rapid Prototyping: Principles and Applications*, Third (3rd) Edition, World Scientific.

Cole, D.P., Riddick, J.C., Jaim, J.C., Strawhecker, K.E. and Zander, N.E. (2016), "Interfacial mechanical behavior of 3D printed ABS", *Journal of Applied Polymer Science*, Vol. 133 No. 30, doi: 10.1002/app.43671.

Costa, S.F., Duarte, F.M. and Covas, J.A. (2011), "Using MATLAB to compute heat transfer in free form extrusion", *MATLAB – A Ubiquitous Tool for the Practical Engineer*, InTech, Rijeka, Croatia, pp. 453-474, (ISBN: 978-953-307-907-3).

Costa, S.F., Duarte, F.M. and Covas, J.A. (2014), "Thermal conditions affecting heat transfer in FDM/FFE: a contribution towards the numerical modelling of the process", *Virtual and Physical Prototyping*, Vol. 10 No. 1, pp. 35-46, doi: 10.1080/17452759.2014.984042.

Costa, S.F., Duarte, F.M. and Covas, J.A. (2015), "An analytical solution for heat transfer during deposition in extrusion-based 3D printing techniques", *in Proceedings of the 15th International Conference Computational and Mathematical Methods in Science and Engineering*, pp. 1161-1172.

Costa, S.F., Duarte, F.M. and Covas, J.A. (2017), "Estimation of filament temperature and adhesion development in fused deposition techniques", *Journal of Materials Processing Technology*, Vol. 245, pp. 167-179, doi: 10.1016/j.jmatprotec.2017.02.026.

Costa, S.F., Duarte, F.M. and Covas, J.A. (2020), "The effect of a phase change during the deposition stage in fused filament fabrication", in Gervasi, O., Murgante, B., Misra, S., GarauIvan, C., Blečić, I., Taniar, D., Apduhan, B., Rocha, A., Tarantino, E., Maria, C., Karaca, T (Eds), *Computational Science and Its Applications – ICCSA 2020*, Springer, pp. 276-285.

D'Amico, A. and Peterson, A.M. (2018), "An adaptable FEA simulation of material extrusion additive manufacturing heat transfer in 3D", *Additive Manufacturing*, Vol. 21, pp. 422-430, doi: 10.1016/j.addma.2018.02.021.

Dutta, D. and Kulkarni, P. (2000), "A review of process planning techniques in layered manufacturing", *Rapid Prototyping Journal*, Vol. 6 No. 1, pp. 16-35, doi: 10.1108/13552540010309859.

Faes, M., Ferrarisa, E. and Moensa, D. (2016), "Influence of inter-layer cooling time on the quasi-static properties of ABS components produced via fused deposition modelling", *Procedia CIRP*, Vol. 42, pp. 748-753, doi: 10.1016/j.procir.2016.02.313.

Ferraris, E., Zhang, J. and Van Hooreweder, B. (2019), "Thermography based in-process monitoring of fused filament fabrication of polymeric parts", *CIRP Annals – Manufacturing Technology*, Vol. 68 No. 1, pp. 213-216, doi: 10.1016/j.cirp.2019.04.123.

Garzon-Hernandez, S., Garcia-Gonzalez, D., Jérusalem, A. and Arias, A. (2020), "Design of FDM 3D printed polymers: an experimental-modelling, methodology for the prediction of mechanical properties", *Materials & Design*, Vol. 188, p. 108414, doi: 10.1016/j.matdes.2019.108414.

Gurrala, P.K. and Regalla, S.P. (2014), "Part strength evolution with bonding between filaments in fused deposition modelling", *Virtual and Physical Prototyping*, Vol. 9 No. 3, pp. 141-149, doi: 10.1080/17452759.2014.913400.

Harris, M., Potgieter, J., Archer, R. and Arif, K.M. (2019), "Effect of material and process specific factors on the strength of printed parts in fused filament fabrication: a review of recent developments", *Materials*, Vol. 12 No. 10, p. 1664, doi: 10.3390/ma12101664.

Holman, J.P. (2010), *Heat Transfer*, McGraw-Hill, New York, NY.

Ingole, D.S., Kuthe, A.M., Thakare, S.B. and Talankar, A.S. (2009), "Rapid prototyping- a technology transfer approach for development of rapid tooling", *Rapid Prototyping Journal*, Vol. 15 No. 4, pp. 280-290, doi: 10.1108/13552540910979794.

Kousiatza, C., Chatzidai, N. and Karalekas, D. (2017), "Temperature mapping of 3D printed polymer plates: experimental and numerical study", *Sensors*, Vol. 17 No. 3, p. 456, doi: 10.3390/s17030456.

Kousiatza, C. and Karalekas, D. (2016), "In-situ monitoring of strain and temperature distributions during fused deposition modeling process", *Materials & Design*, Vol. 97, pp. 400-406, doi: 10.1016/j.matdes.2016.02.099.

Leutenecker-Twelsieka, B., Klahn, C. and Meboldt, M. (2016), "Considering part orientation in design for additive manufacturing", *Procedia CIRP*, Vol. 50, pp. 408-413, doi: 10.1016/j.procir.2016.05.016.

Li, H., Wang, T., Sun, J. and Yu, Z. (2018), "The effect of process parameters in fused deposition modelling on bonding degree and mechanical properties", *Rapid Prototyping Journal*, Vol. 24 No. 1, pp. 80-92, doi: 10.1108/RPJ-06-2016-0090.

Liparoti, S., Sofia, D., Romano, A., Marra, F. and Pantani, R. (2021), "Fused filament deposition of PLA: the role of interlayer adhesion in the mechanical performances", *Polymers*, Vol. 13 No. 3, p. 399, doi: 10.3390/polym13030399.

Mackay, M.E. (2018), "The importance of rheological behavior in the additive manufacturing technique material extrusion", *Journal of Rheology*, Vol. 62 No. 6, pp. 1549-1561, doi: 10.1122/1.5037687.

Malekipoura, E., Attoyeb, S. and El-Mounayri, H. (2018), "Investigation of layer based thermal behavior in fused deposition modeling process by infrared thermography", *Procedia Manufacturing*, Vol. 26, pp. 1014-1022, doi: 10.1016/j.promfg.2018.07.133.

Plaza, E.G., Núñez López, P.J., Torija, M.A. and Muñoz, J. M. (2019), "Analysis of PLA geometric properties processed by FFF additive manufacturing: effects of process parameters and plate-extruder precision motion",

Polymers, Vol. 11 No. 10, p. 1581, doi: 10.3390/polym11101581.

Ravoori, D., Lowery, C., Prajapati, H. and Jain, A. (2019), "Experimental and theoretical investigation of heat transfer in platform bed during polymer extrusion based additive manufacturing", *Polymer Testing*, Vol. 73, pp. 439-446, doi: 10.1016/j.polymertesting.2018.11.025.

Rodriguez, J.F., Thomas, J.P. and Renaud, J.E. (1999), "Maximizing the strength of fused-deposition ABS plastic parts", *10th Solid Freeform Fabrication Symposium*, pp. 335-342. http://dx.doi.org/10.26153/tsw/786

Rodriguez, J.F., Thomas, J.P. and Renaud, J.E. (2000), "Characterization of the mesostructure of fused-deposition acrylonitrile-butadiene-styrene materials", *Rapid Prototyping Journal*, Vol. 6 No. 3, pp. 175-185, doi: 10.1108/13552540010337056.

Rudolph, N., Chen, J. and Dick, T. (2019), "Understanding the temperature field in fused filament fabrication for enhanced mechanical part performance", *AIP Conference Proceedings*, 2055, 140003. 10.1063/1.5084906.

Seppala, J.E. and Migler, K.D. (2016), "Infrared thermography of welding zones produced by polymer extrusion additive manufacturing", *Additive Manufacturing*, Vol. 12, pp. 71-76, doi: 10.1016/j.addma.2016.06.007.

Seppala, J.E., Ha, S.H., Hillgartner, K.E., Davis, C.S. and Migler, B.K. (2017), "Weld formation during material extrusion additive manufacturing", *Soft Matter*, Vol. 13 No. 38, pp. 6761-6769, doi: 10.1039/C7SM00950J.

Spoerk, M., Gonzalez-Gutierrez, J., Sapkota, J., Schuschnigg, S. and Holzer, C. (2018), "Effect of the printing bed temperature on the adhesion of parts produced by fused filament fabrication", *Plastics, Rubber and Composites*, Vol. 47 No. 1, pp. 17-24, doi: 10.1080/14658011.2017.1399531.

Striemann, P., Hülsbusch, D., Niedermeier, M. and Walther, F. (2020), "Optimization and quality evaluation of the interlayer bonding performance of additively manufactured polymer structures", *Polymers*, Vol. 12 No. 5, p. 1166, doi: 10.3390/polym12051166.

Sun, Q., Rizvi, G.M., Bellehumeur, C.T. and Gu, P. (2003), "Experimental study of the cooling characteristics of polymer filaments in FDM and impact on the mesostructures and properties of prototypes", *14th Solid Freeform Fabrication Symposium*, pp 313-323. 10.26153/tsw/5566

Valvez, S., Reis, P.N., Susmel, L. and Berto, F. (2021), "Fused filament fabrication-4D-printed shape memory polymers: a review", *Polymers*, Vol. 13 No. 5, p. 701, doi: 10.3390/polym13050701.

Vanaei, H., Shirinbayan, M., Deligant, M., Raissi, K., Fitoussi, J., Khelladi, S. and Tcharkhtchi, A. (2020), "Influence of process parameters on thermal and mechanical properties of polylactic acid fabricated by fused filament fabrication", *Polymer Engineering & Science*, Vol. 60 No. 8, pp. 1822-1831, doi: 10.1002/pen.25419.

Wang, P., Zou, B. and Ding, S. (2019), "Modeling of surface roughness based on heat transfer considering diffusion among deposition filaments for FDM 3D printing heat-resistant resin", *Applied Thermal Engineering*, Vol. 161, p. 114064, doi: 10.1016/j.applthermaleng.2019.114064.

Wolszczak, P., Lygas, K., Paszko, M. and Wach, R.A. (2018), "Heat distribution in material during fused deposition modelling", *Rapid Prototyping Journal*, Vol. 24 No. 3, pp. 615-622, doi: 10.1108/RPJ-04-2017-0062.

Yang, F. and Pitchumani, R. (2002), "Healing of thermoplastic polymers at an interface under nonisothermal conditions", *Macromolecules*, Vol. 35 No. 8, pp. 3213-3224, doi: 10.1021/ma010858o.

Yardimci, M.A. and Güceri, S. (1996), "Conceptual framework for the thermal process modelling of fused deposition", *Rapid Prototyping Journal*, Vol. 2 No. 2, pp. 26-31, doi: 10.1108/13552549610128206.

Yardimci, M.A., Takeshi, H., Güceri, S. and Danforth, S.C. (1997), "Thermal analysis of fused deposition", *in Proceedings in Solid Freeform Fabrication Symposium, Austin, TX*, pp. 689-698.

Zhang, Y. and Shapiro, V. (2018), "Linear-Time thermal simulation of as-manufactured fused deposition modeling components", *Journal of Manufacturing Science and Engineering*, Vol. 140 No. 7, p. 071002, doi: 10.1115/1.4039556.

Zhou, X., Hsieh, S.J. and Sun, Y. (2017), "Experimental and numerical investigation of the thermal behaviour of polylactic acid during the fused deposition process", *Virtual and Physical Prototyping*, Vol. 12 No. 3, pp. 221-233, doi: 10.1080/17452759.2017.1317214.

Corresponding author

Fernando Moura Duarte can be contacted at: fduarte@dep.uminho.pt